Biosensors and Bioelectronics 84 (2016) 89–96

Contents lists available at ScienceDirect

Biosensors and Bioelectronics

journal homepage: www.elsevier.com/locate/bios

Simultaneous determination of CRP and D-dimer in human blood plasma samples with White Light Reflectance Spectroscopy

Georgios Koukouvinos [a], Panagiota Petrou [a,*], Konstantinos Misiakos [b], Dimitris Drygiannakis [c], Ioannis Raptis [c], Gerasimos Stefanitsis [d], Spyridoula Martini [d], Dimitra Nikita [d], Dimitrios Goustouridis [e], Isabella Moser [f], Gerhard Jobst [f], Sotirios Kakabakos [a]

[a] Immunoassay/Immunosensors Lab, Institute of Nuclear & Radiological Sciences & Technology, Energy & Safety, NCSR "Demokritos", GR-15310 Aghia Paraskevi, Greece
[b] Optical sensors Lab, Institute of Nanoscience and Nanotechnology, NCSR "Demokritos", GR-15310 Aghia Paraskevi, Greece
[c] ThetaMetrisis S.A., Polydefkous 14, GR-12243, Athens, Greece
[d] Diagnostic Laboratories, "Henri Dunant" Hospital, 115 26 Athens, Greece
[e] Electronics Engineering Department, TEI of Piraeus, Athens, Greece
[f] Jobst Technologies GmbH, 79108 Freiburg, Germany

ARTICLE INFO

Article history:
Received 5 October 2015
Received in revised form
27 November 2015
Accepted 30 November 2015
Available online 2 December 2015

Keywords:
Dual-analyte determination
Label-free detection
C-reactive protein
D-dimer
Human blood plasma sample
White light interference spectroscopy

ABSTRACT

A dual-analyte assay for the simultaneous determination of C-reactive protein (CRP) and D-dimer in human blood plasma based on a white light interference spectroscopy sensing platform is presented. Measurement is accomplished in real-time by scanning the sensing surface, on which distinct antibody areas have been created, with a reflection probe used both for illumination of the surface and collection of the reflected interference spectrum. The composition of the transducer, the sensing surface chemical activation and biofunctionalization procedures were optimized with respect to signal magnitude and repeatability. The assay format involved direct detection of CRP whereas for D-dimer a two-site immunoassay employing a biotinylated reporter antibody and reaction with streptavidin was selected. The assays were sensitive with detection limits of 25 ng/mL for both analytes, precise with intra- and inter-assay CV values ranging from 3.6% to 7.7%, and from 4.8% to 9.5%, respectively, for both assays, and accurate with recovery values ranging from 88.5% to 108% for both analytes. Moreover, the values determined for the two analytes in 35 human plasma samples were in excellent agreement with those received for the same samples by standard diagnostic laboratory instrumentation employing commercial kits. The excellent agreement of the results supported the validity of the proposed system for clinical application for the detection of multiple analytes since it was demonstrated that up to seven antibody areas can be created on the sensing surface and successfully interrogated with the developed optical set-up.

1. Introduction

During the thirty years of biosensors development, a wide range of diverse detection principles (electrochemical, optical, micromechanical, etc.) have been designed and boosted in the quest for easy-to-use and low cost devices able for accurate and sensitive detection of various biomarkers (Kuila et al., 2011). Optical biosensing techniques are amongst the more widely used due to the potential for real-time reaction monitoring as well as for multiplexing and miniaturization, two aspects highly desirable for Point-of-Care (PoC) devices (Estevez et al., 2014; Kozma et al., 2014). Despite the fact that the dominating commercially available optical biosensing systems for real-time reaction monitoring are based on SPR (Rich and Myszka, 2010), other optical detection principles are steadily gaining pace including ring resonators (Kindt and Bailey, 2013), waveguide interferometers (Misiakos et al., 2014a, 2014b), and reflectometric interference spectroscopy sensors (Rau and Gauglitz, 2012; Koukouvinos et al., 2015). The latter group of biosensors rely on the interference of reflected light by a stack of transparent layers to monitor in real-time the growing of a biomolecular adlayer due to a specific biorecognition reaction in label-free format. This is achieved by monitoring the changes in the reflected interference patterns caused by the increase in the optical thickness of the biomolecular layer (Özkumur

* Corresponding author.
E-mail address: ypetrou@rrp.demokritos.gr (P. Petrou).

http://dx.doi.org/10.1016/j.bios.2015.11.094
0956-5663/

et al., 2009; Albrecht et al., 2010; Kurihara et al., 2012). Sensing systems based on reflectrometric interference spectroscopy have been applied for the detection of biomarkers, food contaminants, etc., either in single or multi-analyte format. Advantages of this sensing approach are the relatively low cost of instrumentation and operation, the potential for miniaturization of the sensing element and multi-analyte determination, and the feasibility to tailor the system to the requirements of each particular application.

In this work the design and realization of a complete system based on white-light interference spectroscopy suitable for multi-analyte label-free detection of minute concentrations of biomolecules with clinical interest in biological samples (e.g., serum and plasma) is introduced. The bioanalytical system is applied for the simultaneous determination of two markers with prognostic value for myocardial infraction (Lowe et al., 2001; Khawaja and Kullo, 2009), namely C-reactive protein (CRP) and D-dimer, in human blood plasma samples.

CRP is extensively used in clinical practice for diagnosis of inflammatory conditions. Nevertheless, the determination of CRP blood levels (serum or plasma) in combination with causative (high blood pressure, diabetes, high blood cholesterol, smoking) and predisposing factors (obesity, lack of physical activity) is used in prevention programmes to identify patients with high risk for cardiovascular disease (Algarra et al., 2013). Three CRP concentration levels have been proposed in relation to predisposition for cardiovascular disease (Smith et al., 2000; Pearson et al., 2003): low risk (<1 mg/L); average risk (1–3 mg/L); and high risk (>3 mg/L). Due to its high clinical significance and its routine analysis in clinical laboratories a great variety of analytical methodologies have been developed for its determination, the majority of which are immunochemical (Algarra et al., 2013). The methods used range from 96-well plates based ELISA kits (Vashist et al., 2014) to fully automated large volume clinical analyzers (Roberts et al., 2001), and from ultra-high sensitivity sensing platforms (Yeom et al., 2011) to point-of-need portable instruments (Vashist et al., 2015). In addition, significant effort has been put towards the realization of immunosensors for the fast determination of this analyte in serum samples following both labeled and label-free approaches. Most of these sensors have been reviewed in recent publications (Algarra et al., 2013; Chandra et al., 2014), revealing the diversity of the methods involved for the detection of CRP but also the shift of interest to label-free methods aiming to direct and faster analysis. Examples of label-free approaches include sensors based on optical fiber Bragg grating (Sridevi et al., 2015), metal clad waveguide (Kim et al., 2014), SPR (Murata et al., 2013), electrochemistry (Gupta et al., 2014), reflectance interference spectroscopy (Choi et al., 2012) or combination of localized surface plasmon resonance and interference spectroscopy (Yeom et al., 2011). Although some of these sensors present detection sensitivities down to fg/mL (Yeom et al., 2011), none of them has been evaluated using human plasma samples and/or compared with regard to its analytical accuracy with established methods applied in every day clinical practice.

Another marker related to cardiac infarction prognosis is D-dimer. D-dimer is a protein created by degradation of the fibrin molecule (Gaffney 1973, 1993). Elevated levels of D-dimer in blood plasma have been related to severe pathological conditions like pulmonary embolism, septicemia, cirrhosis, carcinoma and sickle cell disease (Raimondi et al., 1993; Wakai et al., 2003). Studies have indicated that D-dimer can be also used as a marker for arterial and venous thrombosis and the prediction of cardiovascular disease. In particular, it has been proposed that blood plasma concentrations over a threshold value of 0.5 mg/mL indicate an increased risk for thrombosis, whereas lower concentrations account for very low risk for a thrombotic episode (Gershlick 1999; Lowe et al., 2001). D-dimer is also determined immunochemically and there are several commercially available kits. However, due to differences in the specificity of the antibodies used, the results obtained from the analysis of patients samples are not interchangeable and they should always compared to results of venography for confirmation of a thrombotic state (Anderson and Wells, 2000; Van der Graff et al., 2000). In addition there are very few reports for D-dimer determination using biosensors based on electrochemical (Chebil et al., 2010), magnetoresistive (Gao et al., 2015) or impedimetric detection (Bourigua et al., 2010) from which only the latter is label-free. In all three cases, a limited number of samples have been employed for the evaluation of the sensor and a moderate matrix effect was observed.

In this work we present for the first time in the literature, at least to our knowledge, the simultaneous determination of C-reactive protein (CRP) and D-dimer in human plasma samples. The determination is achieved by combining a White Light Reflectance Spectroscopy (WLRS) sensing platform with a biochip bearing discrete areas spotted with the analyte specific antibodies. Measurement is accomplished in real-time by precise movement of the sensing surface with respect to the reflection probe used for the white light illumination of the biochip and collection of the reflected light. The WLRS sensing approach has been previously exploited by our group for the real-time and label-free immunochemical determination of different biomarkers such as the complement factor C3b (Petrou et al., 2007) and the total- and free-form of prostate specific antigen in human serum samples (Koukouvinos et al., 2015). Nevertheless, two major improvements are introduced in the present work: (a) the on-chip microfluidic chamber is miniaturized so as to reduce the sample volume from 100 to 20 μl, without reducing the surface area available for biofunctionalization, and (b) the optical set-up was combined with a computer controlled stage which allowed scanning across the long axis of the sensing surface providing for real-time multi-analyte determinations in the same sample. The developed dual-analyte sensing system was evaluated in terms of its analytical characteristics and compared to standard diagnostic laboratory instrumentation using human blood plasma samples.

2. Materials and methods

2.1. Reagents

Four-inch Si wafers ($<100>$) were purchased from Si-Mat Germany (Kaufering, Germany). After cleaning, a 1000-nm thick silicon dioxide layer was grown on the wafers by wet oxidation at 1100 °C in the clean room facility of the Nanotechnology & MEMS Laboratory of Institute of Nanoscience and Nanotechnology of NCSR “Demokritos”. Bovine serum albumin (BSA), (3-aminopropyl)triethoxysilane (APTES), and (3-glycidyloxypropyl)trimethoxysilane (GOPTS) were purchased from Sigma (St. Louis, MO). C-Reactive Protein (CRP) from human fluids, affinity purified polyclonal goat antibody (code GC019) and mouse monoclonal antibody (code MC017) against CRP were from Scripps Laboratories (San Diego, CA). The calibration of CRP standard solutions was performed using a commercially available ELISA kit (hs-CRP; DIAsource Immunoassays S.A., Louvain-la-Neuve, Belgium). D-dimer from human plasma and mouse monoclonal antibodies against D-dimer (code DD2, DD4, DD5, DD6, and DD41) were purchased by HyTest Ltd. (Turku, Finland). Goat polyclonal anti-human D-dimer antibody (MBS857098) was from MyBioSource, Inc. (San Diego, CA). Calibration of D-dimer standard solutions was performed using the D-Dimer BioAssay™ enzyme immunoassay kit (United States Biological, Salem, MA). The succinimidyl-6-(biotinamido)hexanoate (EZ-Link NHS-LC-Biotin) used for the

biotinylation of detection antibodies was from Pierce (Rockford, IL). Biotinylation was performed following a previously published procedure (Koukouvinos et al., 2015). Human blood plasma samples from anonymous donors were provided by the Diagnostic Laboratories of "Henry Dunant" Hospital in Athens, Greece (after approval from the hospital's Ethics Committee and informed consent of the patients). All samples have been previously analyzed using the Siemens Dimension® and Siemens Innovance® Clinical Chemistry System for CRP and D-dimer determination, respectively.

2.2. Sensor surface activation and biofunctionalization

The oxidized silicon wafers were diced in pieces of 75 $(5.0 \times 15)\,mm^2$ prior to chemical activation and biofunctionalization. These dies were cleaned/hydrophilized through treatment with Piranha solution (1:1 H_2SO_4/30% H_2O_2) for 20 min and then washed extensively with distilled water, dried under nitrogen flow and immersed in a 2% (v/v) aqueous APTES solution for 20 min. Then, they were gently washed with distilled water, dried under a nitrogen stream and cured for 20 min at 120 °C. The functionalized dies were kept in a desiccator under vacuum until use. Bands of antibodies against CRP and D-dimer were created on the chips surface by spotting solutions of 200 μg/mL in carbonate buffer, pH 9.2. Each band was created by applying 15×35 overlapping spots with a pitch of 100 μm using a solid pin with a 375-μm tip diameter (SSP015, Arrayit Corporation, Sunnyvale, USA) employing the BioOdyssey Calligrapher™ microarray spotter (Bio-Rad Laboratories, Hercules, CA). Thus, the dimensions of each antibody band were $1.7 \times 3.7\,mm^2$ with a between band interval of 1 mm (Supplementary, Fig. S1A). The chips were kept overnight under controlled humidity conditions (average humidity 75%) and then, they were washed with Tris–HCl 10 mM, pH 8.25, 9 g/L NaCl (washing solution) and immersed in blocking solution (50 mg/mL BSA in 0.1 M $NaHCO_3$, pH 8.5) for 2 h at RT. Finally, the biofunctionalized chips were washed with washing solution and distilled water, dried under nitrogen flow, and used for the assay. The biofunctionalized chip was assembled with an open fluidic compartment cut from a 200-μm thick double side adhesive (Tesa Werk Offenburg GmbH, Germany) and a milled 2-mm thick PMMA cover is applied on top to form the fluidic chamber (Fig. 1A). The PMMA cover material (2-mm thick PLEXIGLAS® GS, casted sheets with superior optical properties, EVONIK Industries, Germany) quality and thickness was carefully selected to facilitate for the probing of light through the external reflection probe (see Section 2.3) and to provide secure sealing. The fluid inlet and outlet has been also embedded on the PMMA top cover (Fig. 1B). Biofunctionalized and packaged chips are mentioned hereafter as biochips.

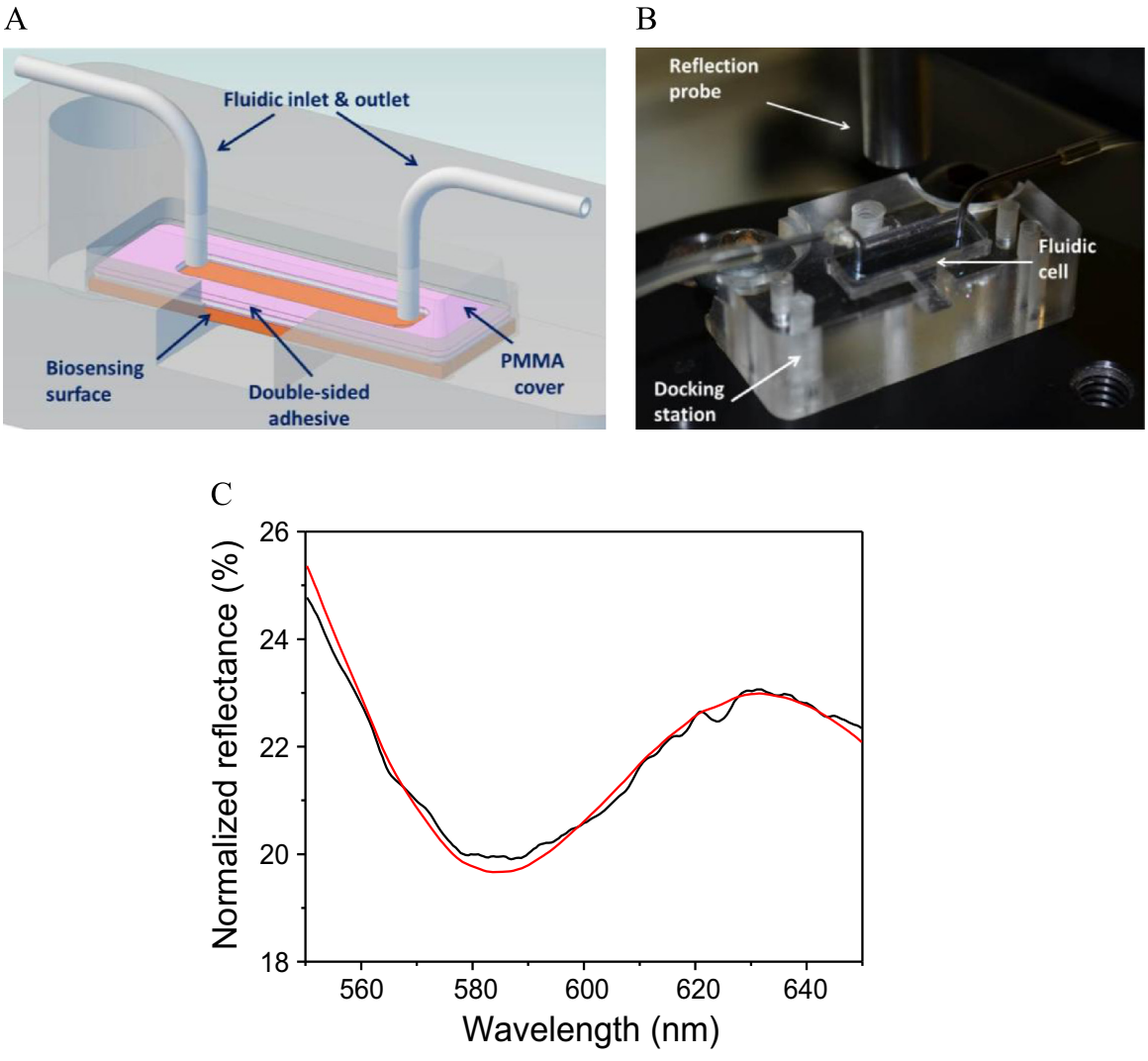

Fig. 1. (A) 3D-schematic of the docking station and the biochip positioning and structure. (B) Photograph of the experimental set-up. Indicated are the reflection probe, the fluidic cell, and the docking station. (C) Typical reflectance spectrum and fitting by the FR-Monitor software.

2.3. Instrumentation

The core hardware elements of the sensing system are the optical setup and the docking station. The biochip is secured on a recess of the PMMA docking station (Fig. 1A and B). The docking station dimensions are 2.0×3.3 cm^2 and the recess is marginally bigger than the biochip (0.5×1.5 cm^2). The optical setup (FR-Basic, ThetaMetrisis) consists of a stabilized for long-term operation visible-near infrared light source (Avalight-Hal; AVANTES Inc., Broomfield, CO, USA), a visible-near infrared spectrometer (Maya 2000 Pro, Ocean Optics), and a commercially available reflection probe (AVANTES Inc., Broomfield, CO, USA). The probe consists of six multi-mode illumination fibers arranged around a central also multi-mode fiber (Supplementary, Fig. S1B). The six illumination fibers guide the light from the light source vertically onto the biochip, which is secured on the docking station, whereas the reflected light is collected by the central fiber and guided to the spectrometer for analysis. The docking station is mounted on a commercially available *X–Y* stage (Prior Ltd, UK) with position accuracy of 10 μm. Reagents were supplied into the on-chip fluidic cell at a constant rate of 20 μl/min employing a standard microsyringe pump (Cole-Palmer, Vernon Hills, IL). All measurements were performed at room temperature using the FR-Monitor software (ThetaMetrisis, Athens, GR) controlling simultaneously both the *X–Y* stage and the optical set-up. The integration time of the spectrometer was set to 15 ms and the reflectance spectrum was recorded every second. The scanning step for the dual-analyte assay was 0.5 mm. A schematic of the biochip with the two antibody bands and its positioning with respect to reflection probe is provided in Supplementary Fig. S1C. The acquired reflectance spectra (arbitrary units) are then transformed to normalized reflectance spectra taking into account the dark and reference spectra from a substrate with known reflectivity (plain Si wafer). The normalized reflectance spectrum is fitted in real-time with the interference equation from two films (SiO_2 and biomolecular adlayer), Fig. 1C, and implemented with the Levenberg-Marquart algorithm (Koukouvinos et al., 2015). Since the SiO_2 layer thickness, measured prior to functionalization, is considered constant, the effective thickness of the adlayer that is formed on top of the biochip due to the biomolecular interactions is measured with high accuracy (Kitsara et al., 2010).

2.4. Dual-analyte assay

The biochips with antibody bands against CRP and D-dimer were loaded on the docking station and secured on the stage. At first, assay buffer (Tris–HCl 50 mM, pH 8.25, 5 mg/mL BSA, 0.5 mg/mL bovine IgG, 9 g/L NaCl) was run through the flow cell. Then, the calibrators containing mixtures of CRP and D-dimer in assay buffer or blood plasma samples diluted with assay buffer were introduced and run for 20 min at a rate of 20 μL/min. After that, a mixture containing 5 μg/mL of anti-CRP antibody and 5 μg/mL of biotinylated anti-D-dimer antibodies in assay buffer was run for 20 min at the same rate, followed by running for 5 min a 5 μg/mL streptavidin solution in the same buffer. A schematic of the assay procedure is provided in Supplementary Fig. S2. The biochip surface was regenerated by running 0.1 M glycine/HCl buffer, pH 2.5, for 5 min, followed by washing and equilibration with assay buffer prior to the next run.

3. Results and discussion

The bioanalytical performance of the proposed biochip depends on various parameters such as the optical properties of the materials of the sensing chip, the surface chemical activation protocol, the biofunctionalization methodology, and the specific antibodies employed. In order to optimize the sensing performance of the proposed system each of these parameters was studied and the optimum conditions were used for the fabrication of the biochips for the simultaneous detection of CRP and D-dimer.

3.1. Selection of the dielectric layer

In WLRS the light travels within the various layers of the biochip and in particular (a) the substrate (Si in our case), (b) the dielectric layer, (c) the biolayers i.e., the immobilized antibody, the analyte bound to the antibody, the reporter antibody layer, and so on, and (d) the cover medium which is the sample under analysis (Supplementary, Fig. S3). The optical properties of these materials affect the overall sensing performance of the biochip. The materials that can be optimized are those for the substrate and the dielectric layer. As it is shown in the supplementary information, the formation of an adlayer on the surface of the dielectric layer causes a shift in the reflectance spectrum that is

$$\delta\lambda = r_1 \frac{1 - r_2^2}{(r_1 + r_2)(1 + r_1 r_2)} \frac{n_1 d_1}{n_2 d_2} \lambda_{0m}$$

where λ_{0m} is the reflectance extremum, r_1 and r_2 the Fresnel coefficients, d_1 and d_2 the thickness, and n_1 and n_2 the refractive index of the biolayer and the dielectric, respectively (Supplementary information, Eq. (10)). The equation above holds also for the shift $\delta\lambda$ caused by an increment of the adlayer thickness d_1 by δd_1, due to the formation of the biolayer and thus d_1 can be replaced by δd_1. As is obvious in this equation, the wavelength shift is independent of the substrate refractive index (n_3), and thus, Si was selected due to the moderate reflectivity in the visible spectral range, the very low roughness that minimize the diffuse reflectance, and of course the potential for mass fabrication of the chips at low cost. At the same time if $n_0 < n_1 < n_2$, then $\delta\lambda$ increases as n_1 approaches n_2 since in such a case r_2 approaches zero. Therefore, the sensitivity increases if the dielectric layer index n_2 is chosen to match the adlayer refractive index n_1. By considering that the refractive index of the biomolecular layers is in the vicinity of 1.46 (Lukosz, 1995), then for a 1-nm hypothetical biomolecular adlayer thickness, the spectral shifts for a dielectric layer made of SiO_2 ($n_2 = 1.46$) and an equivalent layer made of Si_3N_4 ($n_2 = 2.0$), would be 0.6 nm and 0.1 nm, respectively. For this reason, SiO_2 was selected as dielectric layer for the realization of the particular biosensor.

3.2. Chemical activation and biofunctionalization of the sensor surface

The immobilization of biomolecules onto silicon dioxide surfaces requires modification of the surface with a layer that can allow binding either through physisorption or covalent bonding. This step is critical for the development of the assay and four different surface modification approaches have been evaluated in the present work in order to select the optimum one for the development of immunoassays. The first two approaches employ modification with (3-aminopropyl)triethoxysilane (APTES) under aqueous or organic conditions; these surfaces were used for the immobilization of anti-CRP specific antibody through physosorption. The third approach employed two steps: firstly modification with APTES in aqueous environment and then functionalization with glutaraldeyde to introduce groups that could react with the amine-groups of the antibody molecules in order to couple them covalently onto the surface. Similarly, functionalization of the surface with (3-glycidyloxypropyl)trimethoxysilane (GOPTS) resulted in introduction of reactive epoxy-groups onto the silicon

surface that were then used for covalent coupling of the antibodies. In Supplementary Fig. S4, the responses obtained from silicon chips modified following the four protocols upon running a 100 ng/mL CRP solution followed by reaction with anti-CRP antibody are illustrated. From these results, it is obvious that the modification of the sensing surface with an APTES layer deposited through incubation from an aqueous solution provided the highest response during immunoreaction, and was therefore selected for the final application.

3.3. Selection of antibodies

Several antibodies (both polyclonal and monoclonal) for the two analytes have been tested following a non-competitive enzyme immunoassay format. As indicated in Supplementary Fig. S5, best antibody combination for CRP is the goat polyclonal antibody (code GC019) both as capture and reporter antibody, and for D-dimer the goat polyclonal antibody (code MBS857098) as capture with a mixture of two monoclonal antibodies (DD6 and DD41) as reporter ones.

Using the selected capture antibodies, the optimum spotting concentrations for the chips were determined with respect to the signal obtained for various analyte concentrations. In Fig. 2, the responses obtained from biochips coated with anti-CRP solutions at concentrations ranging from 50 to 400 μg/mL for different CRP calibrators are presented. As shown there, the responses obtained for all analyte concentrations increased as the antibody concentration in spotting solution increased from 50 to 200 μg/mL. Further increase of antibody concentration to 400 μg/mL, resulted in a response decrease of at least 50% for all analyte concentrations tested. In fact, the responses obtained were marginally higher ($<20\%$) from those obtained using a concentration of 50 μg/mL in spotting solution. This might be attributed to very compact antibody molecule immobilization that caused strong steric hindrance effects against the relatively bulky analytes. On the other hand, for D-dimer it was found that by increasing of antibody concentration in the spotting solution the specific response was increased and maximum plateau values were reached for antibody concentration in the spotting solution equal to or higher than 200 μg/mL. Thus, this concentration was adopted for the optimization of the assay parameters.

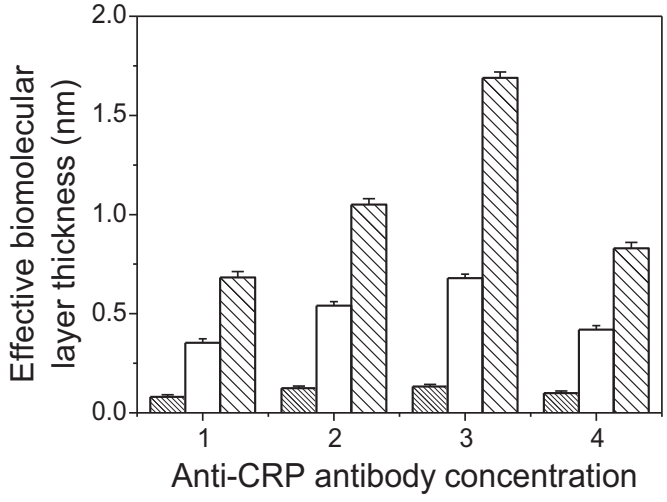

Fig. 2. Effective biomolecular layer thickness values obtained from surfaces coated with anti-CRP antibody solutions with concentration of 50 (1), 100 (2), 200 (3) and 400 μg/mL (4), respectively, for CRP calibrators with concentrations 5 (densely hatched columns), 50 (white columns) and 1000 ng/mL (hatched columns). Detection was performed using a 5 μg/mL reporter antibody solution. Each point is the mean value of 4 replicates ± SD.

3.4. Multi-analyte potential of the sensing platform

The multi-analyte potential of the proposed sensing platform was demonstrated though the simultaneous determination of CRP and D-dimer. This was achieved by immobilizing the respective analyte specific antibodies as discrete bands onto the same surface and scanning the surface with respect to the reflection probe (Supplementary, Fig. S1C). Thus, it was necessary to ensure that the positioning of the biochip after each measuring cycle was precise and allowed for repeatable measurements. In addition, the maximum number and the width of antibody bands that could be accommodated on the particular surface available for scanning ($2.0 \times 7.0\ mm^2$) was determined along with the minimum steps number required to scan the whole spotted area. For this purpose, the anti-CRP antibody was spotted in arrays of bands of different widths and between-band intervals. It was found that in order to have well discriminated responses from the antibody bands that could be also discriminated from that of the intermediate stripes, corresponding to non-specific binding signal, they should have a width of at least 0.5 mm combined with an interval of at least 0.5 mm with a scanning step of 0.25 mm. The responses obtained from a surface spotted according to this scheme are presented in Fig. 3A. The red lines correspond to anti-CRP antibody bands and the black ones to the between-bands intervals. A mean value of 1.28 ± 0.04, with a coefficient of variation (CV) of 3.1%, was determined from the seven bands at the end of the reaction. These values reveal the excellent repeatability of the responses obtained from the different antibody bands. In addition, the responses obtained from the between bands intervals, corresponding to NSB, were negligible and stable throughout the experiment. Thus, with the present chip size, the sensing platform could provide for the simultaneous determination of at least 7 analytes. It should be noted that the signal magnitude was the same with that obtained when measurements were performed without scanning in a biochip with a single wider ($1.7 \times 3.7\ mm^2$) antibody band (Supplementary, Fig. S6).

Five biochips, prepared as described above, were assessed on different days, and the mean responses obtained from the individual bands numbered from 1 to 7 were presented in Fig. 3B. As shown, the repeatability of the measurements was excellent indicating both the good quality of surface modification with the antibodies but also the negligible effect of biochip movement with respect to reflection probe on the repeatability of the measurements. In particular, the CV of the mean values obtained from the same band of the 5 biochips as well as from the 7 bands of each individual surface was less than 5%.

3.5. Dual analyte assay for CRP and D-dimer

The assay format for the dual-analyte assay was determined on the basis of assay sensitivity and working range. In particular, three different approaches were investigated: (a) direct detection of the analytes i.e., by running the calibrators over the biochip, (b) through a sandwich assay format by passing over the chip reporter antibodies after reaction with the analytes and, (c) by running biotinylated reporter antibodies followed by streptavidin. The calibration curves obtained for CRP and D-dimer for each assay configuration are shown in Fig. 4A and B, respectively. The detection limits of the assays were calculated as the concentrations corresponding to +3SD of 20 replicate measurements of zero calibrator (non-specific binding; NSB). For CRP, the detection limit improved from 25 to 2.0, and to 0.05 ng/ml, when detection was performed following the approaches (a), (b) and (c), respectively. At the same time the assay duration was increased from 20 min, to 40 min and finally to 45 min. For D-dimer, on the other hand, detection was possible only by employing a reporter antibody

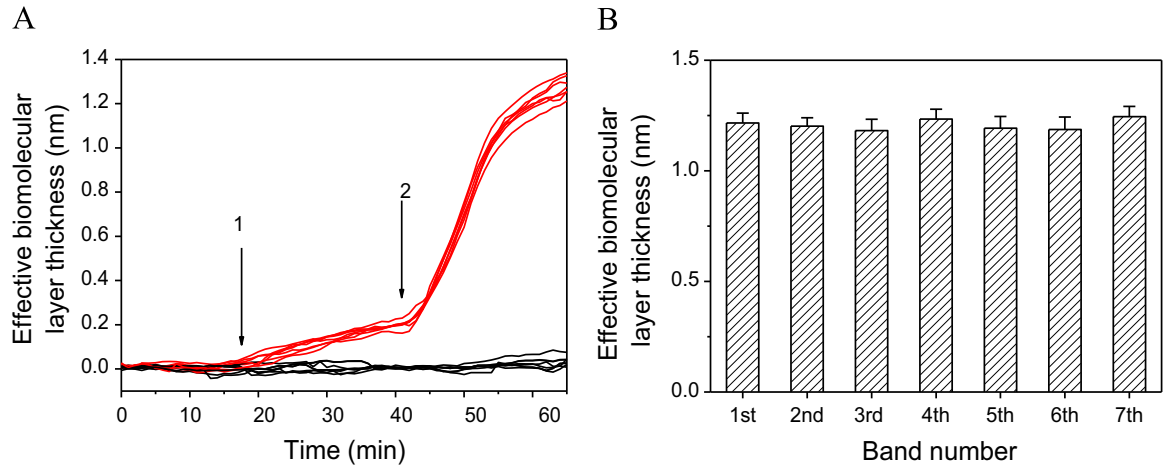

Fig. 3. (A) Effective biomolecular layer thickness monitored in real-time from a surface where 7 anti-CRP antibody bands of 0.5 mm width each (red lines) have been created upon reaction with a calibrator containing 100 μg/mL CRP and (arrow 1) and anti-CRP antibody (arrow 2). The black lines correspond to the responses obtained from the between the anti-CRP antibody bands intervals representing non-specific binding. (B) Mean responses obtained from 5 biochips each one functionalized with 7 anti-CPR antibody bands ± SD. (For interpretation of the references to color in this figure legend, the reader is referred to the web version of this article.)

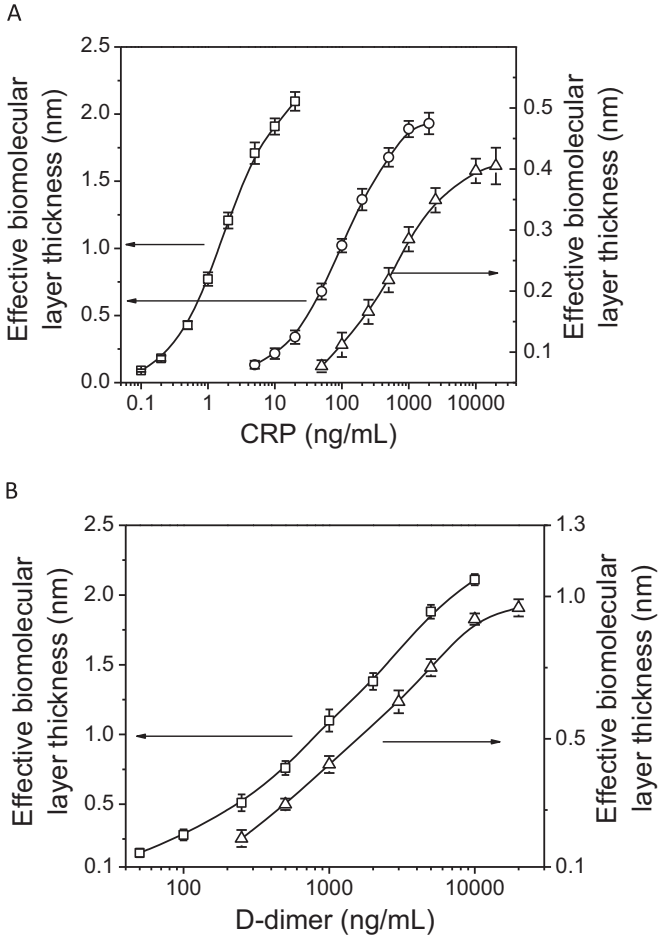

Fig. 4. (A) Typical CRP calibration curves obtained for direct CRP detection (Δ) or using non-biotinylated (○) or biotinylated detection antibody followed by reaction with streptavidin (□). (B) Typical D-dimer calibration curves obtained using non-biotinylated (□) or biotinylated detection antibody followed by reaction with streptavidin (Δ). Each point is the mean value of four measurements ± SD.

either in non-biotinylated form in which case the detection limit was 200 ng/mL or in biotinylated form in which case the detection limit drop to 25 ng/mL when an additional 5-min reaction with streptavidin was employed.

3.6. Effect of plasma dilution

The CRP concentration in the plasma of healthy individuals is usually lower than 5 μg/mL; however, in inflammatory conditions concentrations in the range of 100–400 μg/mL or even higher are frequently determined. Nevertheless, the detection of CRP concentrations lower than 5 μg/mL is also desirable, in order to classify a patient as low, medium or high risk for myocardial infarction. Similarly, the D-dimer concentration in the plasma of healthy individuals should be lower than 0.5 μg/mL; but its concentration in plasma could increase up to several μg/mL in pathological conditions. To be able to cover the extended CRP and D-dimer concentrations that should be measured in plasma, dilution of the sample is usually employed. Thus, the ability of the sensor to provide reliable results for a wide range of plasma dilutions was investigated using pooled human plasma free of CRP and D-dimer spiked with appropriate amounts of these two analytes. The spiking levels were selected so as after 20, 50, 100, 200 and 1000-times dilution with assay buffer, the final CRP and D-dimer concentration to be in all cases 100 and 500 ng/mL, respectively. The responses obtained when these samples were analyzed are depicted in Supplementary Fig. S7, along with the response received from the respective calibrator prepared in buffer. As it is shown, the responses obtained for all plasma dilutions were the same with the response provided from the calibrator in buffer, indicating no interference from blood plasma for all the dilutions tested.

3.7. Repeatability and accuracy of on-chip assays

The developed assays repeatability and accuracy were also evaluated. The repeatability was assessed by running three control samples prepared in analyte-free plasma and corresponding to three different concentration levels of analyte (5, 20 and 100 μg/mL for CRP; 10, 50, and 200 μg/mL for D-dimer) 3 times within the same day as well as for at least 20 runs in different days and employing a 50-times plasma dilution. The intra-assay CV values ranged from 3.6 to 7.7%, whereas the inter-assay CV values from 4.8 to 9.5%, for both assays. The accuracy of the assays was evaluated through recovery experiments. For this purpose, three plasma blood samples from anonymous donors were spiked with known concentrations of CRP and D-dimer and the concentration of both analytes in each sample was determined both prior to and after the exogenous analyte addition. Due to the different concentration ranges of CRP and D-dimer in human plasma and the

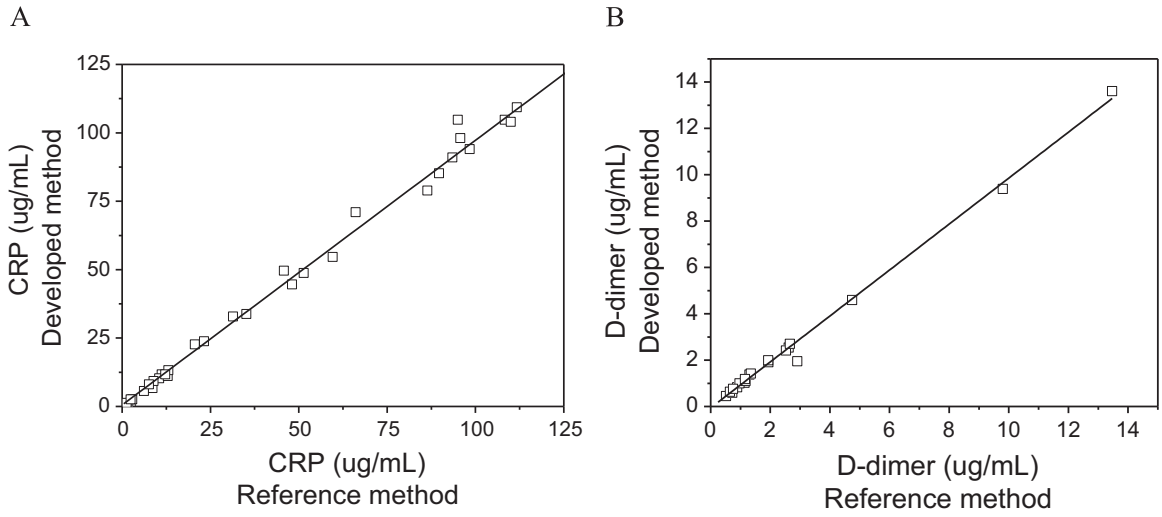

Fig. 5. Correlation of (A) CRP and (B) D-dimer concentrations determined in blood plasma samples from 35 anonymous donors by a diagnostics laboratory methods with those provided for the same samples by the dual-analyte sensor developed.

different working ranges of the calibration curves, for the simultaneous determination of two analytes in the recovery experiments a 50-times dilution was applied. The determination of CRP was based on the direct assay format, i.e., without using the reporter antibody, whereas the D-dimer was determined after reaction with biotinylated reporter antibody and streptavidin. Percent recovery was calculated as the ratio of the added amount determined to the actual amount added in the sample. The results provided in Supplementary Table S1 show that the recovery values ranged from 88.5 to 108%.

Furthermore, the accuracy of the developed dual-analyte assay was evaluated by analysing 35 human blood plasma samples from anonymous donors previously analyzed at the Diagnostic Laboratories of Henry Dunant Hospital using the Siemens Dimension® and Siemens Innovance® analyzer for CRP and D-dimer determination, respectively. As it can be concluded from Fig. 5, there was a very good agreement between the values determined with the clinical laboratory method and those determined for the same samples with the sensor developed. The equation of the correlation linear regression curves was $y=0.981(\pm 0.014)\ x+0.05\ (\pm 0.75)$ for CRP and $y=0.991(\pm 0.02)\ x+0.06(\pm 0.07)$ for D-dimer, respectively, and the correlation co-efficient was $r^2=0.997$ for CRP and $r^2=0.998$ for D-dimer. It should be noted that for each sample a first 20-times dilution was employed and depending on the concentration determined further dilution was applied in order for the final concentration to fall within the linear range of the calibration curve. Overall the assay developed was repeatable and accurate and could be used for the determination of CRP and D-dimer levels in human plasma samples over a wide range of concentrations.

3.8. Stability of biofunctionalized surfaces towards regeneration and storage

Another important issue is the stability of the biomolecules immobilized on the transducer surface. The stability of the antibody-functionalized surfaces was determined by repetitive regeneration-assay cycles performed on the same biochip in four consecutive days (see Supplementary, Fig. S8) as well as by testing different biochips kept dry in desiccator over a period of one month (Supplementary, Fig. S9). It was found that the CRP antibody could afford more than 40 regeneration cycles performed within 4 days, whereas the D-dimer antibody could be regenerated for up to 25 times. Concerning the dried biochips, it was found that the immobilized antibodies for CRP and D-dimer were stable for two weeks. It should be noted, that no special treatment of the biochips, other than blocking and washing, was performed in order to stabilize the immobilized antibodies. Such treatments are available and could be further improve the performance of the proposed sensing platform.

A comparison of the analytical performance of the dual-analyte assay with other sensing systems relying on label-free assay formats for the simultaneous determination of the specific analytes, namely CRP and D-dimer, is provided in Table 1. As shown, there are only two reports where the concentration of CRP and D-dimer biomarkers is determined on the same biochip. The first report concerns a surface acoustic wave sensor (SAW) complemented with a fluidic that allows detection in sequence of four cardiac markers, amongst them CRP and D-dimer. Detection is performed directly by passing calibrators of the analytes separately onto the respective channels for 220 s for CRP and 600 s for D-Dimer, respectively. The detection limits are not mentioned only the assays dynamic range. Compared to this sensor, our system has approximately 5- and 40-times lower quantification limits for CRP and D-dimer, respectively; however, the assay time of the proposed sensor is approx. 3-times longer. In addition, the SAW system performance has not been tested with real human plasma samples. The second report (Furin et al., 2011) refers to the application of a point-of-care system based on Reflectometric Interference Spectroscopy (RIfS) for the determination of these two

Table 1
Comparison of analytical characteristics of the developed sensing platform with other label-free sensing systems.

Sensing platform	Analyte	Detection limit	Dynamic range	Assay duration	Analysis of real samples
Proposed sensor	CRP	25 ng/mL	0.05–2.5 μg/mL	45 min	Yes
	D-dimer	25 ng/mL	0.05–1.0 μg/mL		
Surface acoustic wave (Mitsakakis and Gizeli, 2011)	CRP	n.m.*	0.25–20 μg/mL	~14 min	No
	D-dimer	n.m.	2.0–10 μg/mL		
RIfS (Furin et al., 2011)	CRP	n.m.	n.m.	Few sec	No
	D-dimer	n.m.	n.m.		

* n.m.=non mentioned.

analytes; however, the only data provided refer to a D-dimer concentration of 5 μg/mL and two concentrations of CRP; 0.2 and 325 μg/mL. Thus, direct comparison with the proposed system is not possible.

4. Conclusions

The development of a dual-analyte sensor for the simultaneous determination of C-reactive protein and D-dimer in human blood plasma samples based on a white light interference spectroscopy sensing platform is presented. Dual-analyte determinations are realized by creating distinct antibody bands on the sensing surface which is scanned with a reflection probe that provides both for illumination with broad-band light and collection of the reflected interference spectrum. The composition of the transducer, the sensing surface chemical activation and biofunctionalization procedures, as well as the assay format for each analyte were optimized with respect to signal magnitude, repeatability of the measurements and the expected concentrations of the two analytes in human blood plasma samples. For CRP, direct detection was adequate for the analysis of blood plasma samples, whereas for D-dimer a two-step sandwich immunoassay with a biotinylated reporter antibody combined with streptavidin was necessary in order to achieve the required detection sensitivity. Both assays were precise and accurate and provided blood plasma values for both analytes that were in excellent agreement with those received for the same samples by standard diagnostic laboratory techniques. The overall results supported the validity of the proposed system for determination of multiple-analytes in clinical samples since it was demonstrated that up to seven antibody areas can be created on the same sensing surface and successfully interrogated with the developed optical set-up. Taking into account the small size and low cost of biochip fabrication, its multi-analyte and regeneration potential, the low instrumentation cost along with its analytical capabilities, the proposed sensing platform should find wide application in clinical diagnostics, food analysis and environmental monitoring.

Acknowledgment

The authors acknowledge funding from the Greek General Secretariat for Research and Technology and the European Regional Development Fund under the Action “Development Grants for Research Institutions–KRIPIS” (Contract number MIS 452090) of OPCE II.

Appendix A. Supplementary material

Supplementary data associated with this article can be found in the online version at http://dx.doi.org/10.1016/j.bios.2015.11.094.

References

Albrecht, C., Fechner, P., Honcharenko, D., Baltzer, L., Gauglitz, G., 2010. Biosens. Bioelectron. 25, 2302–2308.
Algarra, M., Gomes, D., Esteves da Silva, J.C.G., 2013. Clin. Chim. Acta 415, 1–9.
Anderson, D.R., Wells, P.S., 2000. Curr. Opin. Hematol. 7, 296–301.
Bourigua, S., Hnaien, M., Bessueille, F., Lagarde, F., Dzyadevych, S., Maaref, A., Bausells, J., Errachid, A., Jaffrezi Renault, N., 2010. Biosens. Bioelectron. 26, 1278–1282.
Chandra, P., Suman, P., Airon, H., Mukherjee, M., Kumar, P., 2014. World J. Methodol. 26, 1–5.
Chebil, S., Hafaiedh, I., Sauriat-Dorizon, H., Jaffrezi-Renault, N., Errachid, A., Ali, Z., Korri-Youssoufi, H., 2010. Biosens. Bioelectron. 26, 736–742.
Choi, H.W., Sakata, Y., Kurihara, Y., Ooya, T., Takeuchi, T., 2012. Anal. Chim. Acta 728, 64–68.
Estevez, M.-C., Otte, M.A., Sepulveda, B., Lechuga, L.M., 2014. Anal. Chim. Acta 806, 55–73.
Furin, D., Sämann, M., Proll, G., Schubert, M., Gauglitz, G., 2011. Procedia Eng. 25, 80–83.
Gaffney, P.J., 1973. Thromb. Res. 2, 201–218.
Gaffney, P.J., 1993. Fibrinolysis 7, 2–8.
Gao, Y.-Z., Zhang, L., Huo, W.-S., Shi, S., Lian, J., Gao, Y.-H., 2015. J. Anal. Chem. 43, 802–807.
Gershlick, H.A., 1999. Eur. Heart J. 20, 1443–1444.
Gupta, R.K., Periyakaruppan, A., Meyyappan, M., Koehne, J.E., 2014. Biosens. Bioelectron. 59, 112–119.
Kindt, J.T., Bailey, R.C., 2013. Curr. Opin. Chem. Biol. 17, 818–826.
Khawaja, F.J., Kullo, I.J., 2009. Vasc. Med. 14, 381–392.
Kim, B.B., Im, W.J., Byun, J.Y., Kim, H.M., Kim, M.-G., Shina, Y.-B., 2014. Sens. Actuators B 190, 243–248.
Kitsara, M., Petrou, P., Kontziampasis, D., Misiakos, K., Makarona, E., Raptis, I., Beltsios, K., 2010. Microelectron. Eng. 87, 802–805.
Koukouvinos, G., Petrou, P.S., Misiakos, K., Drygiannakis, D., Raptis, I., Goustouridis, D., Kakabakos, S.E., 2015. Sens. Actuators B 209, 1041–1048.
Kozma, P., Kehl, F., Ehrentreich-Förster, E., Stamm, C., Bier, F.F., 2014. Biosens. Bioelectron. 58, 287–307.
Kuila, T., Bose, S., Khanra, P., Mishra, A.K., Kim, N.H., Lee, J.H., 2011. Biosens. Bioelectron. 26, 4637–4648.
Kurihara, Y., Takama, M., Sekiya, T., Yoshihara, Y., Ooya, T., Takeuchi, T., 2012. Langmuir 28, 13609–13615.
Lowe, G.D.O., Yarnell, J.W., Rumley, A., Bainton, D., Sweetnam, P.M., 2001. Arterioscler. Thromb. Vasc. Biol. 21 (2001), 603–610.
Lukosz, W., 1995. Sens. Actuators B 29, 37–50.
Misiakos, K., Raptis, I., Salapatas, A., Makarona, E., Botsialas, A., Hoekman, M., Stoffer, R., Jobst, G., 2014a. Opt. Express 22, 8856–8870.
Misiakos, K., Raptis, I., Makarona, E., Botsialas, A., Salapatas, A., Oikonomou, P., Psarouli, A., Petrou, P.S., Kakabakos, S.E., Tukkiniemi, K., Sopanen, M., Jobst, G., 2014b. Opt. Express 22, 26803–26813.
Mitsakakis, K., Gizeli, E., 2011. Anal. Chim. Acta 699, 1–5.
Murata, A., Ooya, T., Takeuchi, T., 2013. Biosens. Bioelectron. 43, 45–49.
Özkumur, E., Yalcin, A., Cretich, M., Lopez, C.A., Bergstein, D.A., Goldberg, B.B., Chiari, M., Ünlü, M.S., 2009. Biosens. Bioelectron. 25, 167–172.
Pearson, T.A., Mensah, G.A., Alexander, R.W., Anderson, J.L., Cannon, R.O., 2003. Circulation 107, 499–511.
Petrou, P.S., Chatzichristidi, M., Douvas, A.M., Argitis, P., Misiakos, K., Kakabakos, S. E., 2007. Biosens. Bioelectron. 22, 1994–2002.
Raimondi, P., Bongard, O., de Moerloose, P., Reber, G., Waldvogel, F., Bounameaux, H., 1993. Thromb. Res. 69, 125–130.
Rau, S., Günter Gauglitz, G., 2012. Anal. Bioanal. Chem. 402, 529–536.
Rich, R.L., Myszka, D.G., 2010. J. Mol. Recognit. 23, 1–64.
Roberts, W.L., Moulton, L., Law, T.C., Farrow, G., Cooper-Anderson, M., Savory, J., Rifai, N., 2001. Clin. Chem. 47, 418–425.
Smith, S.C., Greenland, P., Grundy, S.M., 2000. Circulation 101, 111–116.
Sridevi, S., Vasu, K.S., Asokan, S., Sood, A.K., 2015. Biosens. Bioelectron. 65, 251–256.
Yeom, S.-H., Ok-Geun Kim, O.-G., Kang, B.-H., Kim, K.-J., Yuan, H., Kwon, D.H., Kim, H.-R., Kang, S.-W., 2011. Opt. Express 19, 22882–22891.
Van der Graff, F., van den Borne, H., van der Kolk, M., de Wild, P.J., Janssen, G.W., van Uum, S.H., 2000. Thromb. Haemost. 83, 191–198.
Vashist, S.K., Czilwik, G., van Oordt, T., von Stetten, F., Zengerle, R., Schneider, M., Luong, J.H.T., 2014. Anal. Biochem. 456, 32–37.
Vashist, S.K., van Oordt, T., Schneider, M., Zengerle, R., von Stetten, F., Luong, J.H.T., 2015. Biosens. Bioelectron. 67, 248–255.
Wakai, A., Gleeson, A., Winter, D., 2003. Emerg. Med. J. 20, 319–325.